

The cylindrical bending vibration of a laminated elastic plate due to piezoelectric actuators

J S Yang†, R C Batra‡ and X Q Liang‡

† Department of Mechanical Engineering, Aeronautical Engineering and Mechanics, Rensselaer Polytechnic Institute, Troy, NY 12180, USA

‡ Department of Engineering Science and Mechanics, Virginia Polytechnic Institute and State University, Blacksburg, VA 24061-0219, USA

Received 12 May 1994, accepted for publication 16 August 1994

Abstract. We analyze the forced cylindrical bending vibrations of a laminated elastic plate with actuators at the top and bottom surfaces and forced into vibrations by applying time harmonic voltages to the actuators. The actuators are modeled as thin films and mixed edge conditions are employed to simulate simple supports. The analysis is performed by using the method of Fourier series and the solution is exact within the assumptions of linear elasticity and plane strain deformations. Numerical results are computed for an aluminum plate with actuators affixed to its two major surfaces.

1. Introduction

Elastic beams or plates with piezoelectric films attached to them have been of great interest because of their use as smart structures. Most analytical analyses have been based on various approximate beam or plate theories [1].

Pagano [2] has used the method of Fourier series to study the cylindrical bending of a simply supported elastic composite plate. The solution is exact within the assumptions of plane strain deformations and linear theory of elasticity. The series solution satisfies boundary conditions for a simply supported plate characterized by the vanishing deflection and bending moments at the edges. Ray *et al* [3] generalized Pagano's result to analyze the cylindrical bending of a simply supported piezoelectric plate, and later [4] the cylindrical bending of an elastic plate with piezoelectric layers affixed to the bottom and top surfaces. Recently, Zhou and Tiersten [5] have used the Fourier series method to analyze the cylindrical bending of a laminated elastic plate with actuators on the bottom and top surfaces. The above analyses are all for static bending problems.

In this paper, the Fourier series method is employed to study the cylindrical bending vibration of a simply supported elastic plate with piezoelectric actuators under time harmonic driving voltages. The laminated elastic plate can be made of either an isotropic or orthotropic material. Numerical results for an example problem are given.

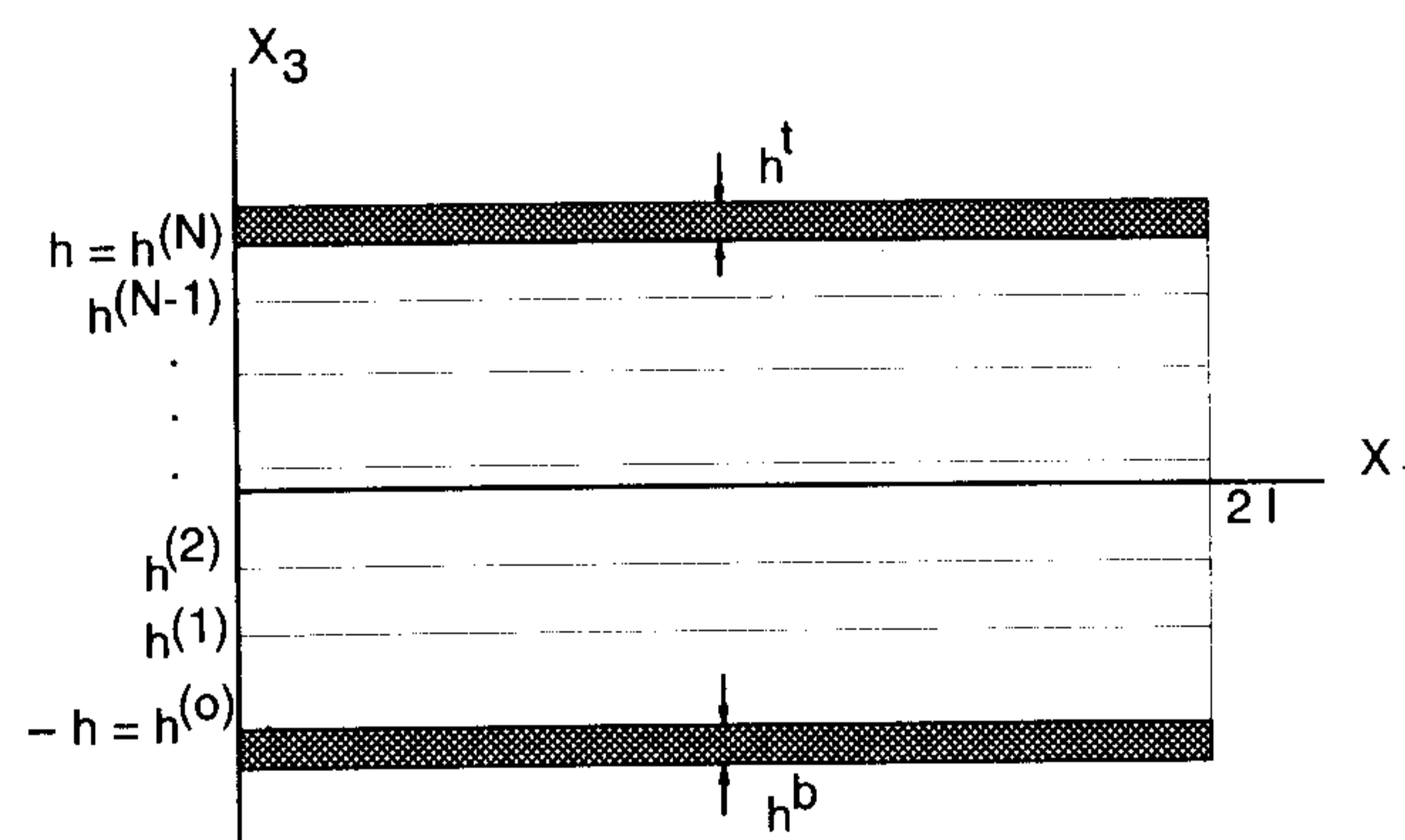


Figure 1. An N -layer elastic plate with piezoelectric actuators at the bottom and top surfaces.

2. Governing equations

We consider an N -layer laminated elastic plate of length $2l$ and total thickness $2h$ with piezoelectric film actuators attached to its bottom $x_3 = -h$ and top $x_3 = h$ surfaces, as shown in figure 1. The positions of the bottom and top surfaces of the plate as well as of the $N - 1$ interfaces are denoted by $h^{(0)} = -h, h^{(1)}, \dots, h^{(N-1)}, h^{(N)} = h$ respectively. The plate is forced into cylindrical bending vibrations with $u_2 = 0$ and $\partial/\partial x_2 = 0$ by applying voltages to the actuators.

2.1. Governing equations

For the n th layer ($n = 1, 2, 3, \dots, N$) of the plate, the relevant equations of motion in rectangular Cartesian

coordinates are

$$\begin{aligned}\tau_{11,1}^{(n)} + \tau_{31,3}^{(n)} &= \rho^{(n)} \ddot{u}_1^{(n)} \\ \tau_{13,1}^{(n)} + \tau_{33,3}^{(n)} &= \rho^{(n)} \ddot{u}_3^{(n)}\end{aligned}\quad (1)$$

where a superscript n in the parenthesis indicates quantities for the n th layer, a superimposed dot indicates partial differentiation with respect to time t and a comma followed by an index i signifies partial differentiation with respect to x_i . Furthermore ρ is the mass density, τ_{ij} the stress tensor and u_i the displacement of a material point. The relevant constitutive equations for an orthotropic material are

$$\begin{aligned}\tau_{11}^{(n)} &= c_{11}^{(n)} u_{1,1}^{(n)} + c_{13}^{(n)} u_{3,3}^{(n)} \\ \tau_{33}^{(n)} &= c_{13}^{(n)} u_{1,1}^{(n)} + c_{33}^{(n)} u_{3,3}^{(n)} \\ \tau_{31}^{(n)} &= c_{55}^{(n)} (u_{3,1}^{(n)} + u_{1,3}^{(n)})\end{aligned}\quad (2)$$

which can be reduced to those for an isotropic material. Here $c_{11}^{(n)}$, $c_{13}^{(n)}$, $c_{33}^{(n)}$, and $c_{55}^{(n)}$ are elasticities for the material of the n th layer. The boundary conditions for each layer at both ends are

$$\tau_{11}^{(n)} = 0 \quad u_3^{(n)} = 0 \quad \text{at } x_1 = 0, 2l. \quad (3)$$

We note that these simulate a simply supported plate characterized by the vanishing of the deflection and bending moment at both ends. At the interface $h^{(n)}$ between the n th and $(n+1)$ th layers, we have

$$\begin{aligned}\tau_{31}^{(n)} &= \tau_{31}^{(n+1)}, \quad \tau_{33}^{(n)} = \tau_{33}^{(n+1)} \quad \text{at } x_3 = h^{(n)} \\ u_1^{(n)} &= u_1^{(n+1)}, \quad u_3^{(n)} = u_3^{(n+1)} \quad \text{at } x_3 = h^{(n)}\end{aligned}\quad (4)$$

That is, the displacement and tractions are continuous across the interface between the n th and $(n+1)$ th layer. Similar conditions hold at the interface $h^{(n-1)}$ between the n th and $(n-1)$ th layer. In terms of displacements, (1), (3) and (4) can be written as

$$\begin{aligned}c_{11}^{(n)} u_{1,11}^{(n)} + c_{55}^{(n)} u_{1,33}^{(n)} + (c_{13}^{(n)} + c_{55}^{(n)}) u_{3,13}^{(n)} &= \rho^{(n)} \ddot{u}_1^{(n)} \\ (c_{13}^{(n)} + c_{55}^{(n)}) u_{1,13}^{(n)} + c_{55}^{(n)} u_{3,11}^{(n)} + c_{33}^{(n)} u_{3,33}^{(n)} &= \rho^{(n)} \ddot{u}_3^{(n)} \\ c_{11}^{(n)} u_{1,1}^{(n)} + c_{13}^{(n)} u_{3,3}^{(n)} &= 0 \quad \text{at } x_1 = 0, 2l \\ u_3^{(n)} &= 0 \quad \text{at } x_1 = 0, 2l\end{aligned}\quad (5)$$

and

$$\begin{aligned}c_{55}^{(n)} (u_{3,1}^{(n)} + u_{1,3}^{(n)}) &= c_{55}^{(n+1)} (u_{3,1}^{(n+1)} + u_{1,3}^{(n+1)}) \\ \text{at } x_3 &= h^{(n)} \\ c_{13}^{(n)} u_{1,1}^{(n)} + c_{33}^{(n)} u_{3,3}^{(n)} &= c_{13}^{(n+1)} u_{1,1}^{(n+1)} \\ &+ c_{33}^{(n+1)} u_{3,3}^{(n+1)} \quad \text{at } x_3 = h^{(n)} \\ u_1^{(n)} &= u_1^{(n+1)}, \quad u_3^{(n)} = u_3^{(n+1)} \quad \text{at } x_3 = h^{(n)}\end{aligned}\quad (6)$$

The piezoelectric actuators are modeled by the equations for a thin piezoelectric film [6]. We use

a superscript b to indicate quantities for the bottom actuator with mass density ρ^b , thickness h^b and displacement $u_1^b(x_1, t)$. The balance of linear momentum in the x_1 direction yields

$$h^b \tau_{11,1}^b + \tau_{31}^{(1)} \Big|_{x_3=-h} = \rho^b h^b \ddot{u}_1^b. \quad (7)$$

For polarized ceramics poled in the x_3 direction, the constitutive equations which satisfy the electric charge equation to the lowest order are

$$\tau_{11}^b = \bar{c}_{11}^b u_{1,1}^b - \bar{e}_{31}^b E_3^b = \bar{c}_{11}^b u_{1,1}^b - \bar{e}_{31}^b V^b(t)/h^b \quad (8)$$

where

$$\begin{aligned}\bar{c}_{11}^b &= s_{11}^b/\Delta, \quad \bar{e}_{31}^b = d_{31}^b/(s_{11}^b + s_{12}^b) \\ \Delta &= s_{11}^b s_{11}^b - s_{12}^b s_{12}^b\end{aligned}\quad (9)$$

or

$$\bar{c}_{11}^b = c_{11}^b - c_{13}^b c_{13}^b / c_{33}^b, \quad \bar{e}_{31}^b = e_{31}^b - e_{33}^b c_{13}^b / c_{33}^b. \quad (10)$$

In (8) we have set $E_3^b = V^b(t)/h^b$ where $V^b(t)$ is the applied time dependent voltage across the bounding surfaces of the bottom actuator. In equations (9) and (10), s_{11}^b , s_{12}^b , and d_{31}^b are the elastic and piezoelectric constants for the actuator material. The end conditions for the bottom actuator are

$$\tau_{11}^b = 0 \quad \text{at } x_1 = 0, 2l \quad (11)$$

In terms of displacements, (7) and (11) can be written as

$$\begin{aligned}h^b \bar{c}_{11}^b u_{1,11}^b + c_{55}^{(1)} (u_{3,1}^{(1)} + u_{1,3}^{(1)}) \Big|_{x_3=-h} &= \rho^b h^b \ddot{u}_1^b \\ \bar{c}_{11}^b u_{1,1}^b &= \bar{e}_{31}^b V^b(t)/h^b \quad \text{at } x_1 = 0, 2l\end{aligned}\quad (12)$$

Similarly, the superscript t is used to denote quantities for the top actuator. We have

$$h^t \tau_{11,1}^t - \tau_{31}^{(N)} \Big|_{x_3=h} = \rho^t h^t \ddot{u}_1^t \quad (13)$$

$$\tau_{11}^t = \bar{c}_{11}^t u_{1,1}^t - \bar{e}_{31}^t E_3^t = \bar{c}_{11}^t u_{1,1}^t - \bar{e}_{31}^t V^t(t)/h^t \quad (14)$$

in which we have set $E_3^t = V^t(t)/h^t$. The end conditions for the top actuator are

$$\tau_{11}^t = 0 \quad \text{at } x_1 = 0, 2l \quad (15)$$

In terms of displacements, (13) and (15) become

$$\begin{aligned}h^t \bar{c}_{11}^t u_{1,11}^t - c_{55}^{(N)} (u_{3,1}^{(N)} + u_{1,3}^{(N)}) \Big|_{x_3=h} &= \rho^t h^t \ddot{u}_1^t \\ \bar{c}_{11}^t u_{1,1}^t &= \bar{e}_{31}^t V^t(t)/h^t \quad \text{at } x_1 = 0, 2l\end{aligned}\quad (16)$$

The additional boundary conditions at the top and bottom surfaces of the laminated plate are given by

$$\begin{aligned}\tau_{33}^{(1)} &= \rho^b h^b \ddot{u}_3^{(1)}, \quad u_1^{(1)} = u_1^b \quad \text{at } x_3 = -h \\ -\tau_{33}^{(N)} &= \rho^t h^t \ddot{u}_3^{(N)}, \quad u_1^{(N)} = u_1^t \quad \text{at } x_3 = h\end{aligned}\quad (17)$$

which, when written in terms of displacements, become

$$\begin{aligned} c_{13}^{(1)} u_{1,1}^{(1)} + c_{33}^{(1)} u_{3,3}^{(1)} &= \rho^b h^b \ddot{u}_3^{(1)}, & u_1^{(1)} &= u_1^b \\ \text{at } x_3 &= -h \\ - (c_{13}^{(N)} u_{1,1}^{(N)} + c_{33}^{(N)} u_{3,3}^{(N)}) &= \rho^t h^t \ddot{u}_3^{(N)}, & u_1^{(N)} &= u_1^t \\ \text{at } x_3 &= h \end{aligned} \quad (18)$$

Equations (17) follow from the continuity of tractions and displacements at the interface between the actuator and the plate, and incorporate the balance of linear momentum, in the x_3 direction, for the actuator. The complete set of equations and boundary conditions consists of equations (5) for each of the N layers, equations (6) for each of the $N - 1$ interfaces, and equations (12), (16) and (18).

2.2. Time harmonic vibrations

We study vibrations of the plate under time harmonic driving voltage

$$\begin{aligned} V^b(t) &= \bar{V}^b e^{i\omega t} \\ V^t(t) &= \bar{V}^t e^{i\omega t} \end{aligned} \quad (19)$$

where \bar{V}^b and \bar{V}^t are constants. Accordingly, for steady state vibrations, all the field quantities have the same time dependence

$$\begin{aligned} u_1^{(n)}(x_1, x_3, t) &= \tilde{u}_1^{(n)}(x_1, x_3) e^{i\omega t} \\ u_3^{(n)}(x_1, x_3, t) &= \tilde{u}_3^{(n)}(x_1, x_3) e^{i\omega t} \\ u_1^b(x_1, t) &= \tilde{u}_1^b(x_1) e^{i\omega t} \\ u_1^t(x_1, t) &= \tilde{u}_1^t(x_1) e^{i\omega t}. \end{aligned} \quad (20)$$

Henceforth, we drop the superimposed tildes. Substitution of (20) into (5), (6), (12), (16) and (18) yields

$$\begin{aligned} c_{11}^{(n)} u_{1,1}^{(n)} + c_{55}^{(n)} u_{1,33}^{(n)} + (c_{13}^{(n)} + c_{55}^{(n)}) u_{3,13}^{(n)} &= -\rho^{(n)} \omega^2 u_1^{(n)} \\ (c_{13}^{(n)} + c_{55}^{(n)}) u_{1,13}^{(n)} + c_{55}^{(n)} u_{3,11}^{(n)} + c_{33}^{(n)} u_{3,33}^{(n)} &= -\rho^{(n)} \omega^2 u_3^{(n)} \\ c_{11}^{(n)} u_{1,1}^{(n)} + c_{13}^{(n)} u_{3,3}^{(n)} &= 0 \quad \text{at } x_1 = 0, 2l \\ u_3^{(n)} &= 0 \quad \text{at } x_1 = 0, 2l \end{aligned} \quad (21)$$

$$\begin{aligned} c_{55}^{(n)} (u_{3,1}^{(n)} + u_{1,3}^{(n)}) &= c_{55}^{(n+1)} (u_{3,1}^{(n+1)} + u_{1,3}^{(n+1)}) \\ \text{at } x_3 &= h^{(n)} \\ c_{13}^{(n)} u_{1,1}^{(n)} + c_{33}^{(n)} u_{3,3}^{(n)} &= c_{13}^{(n+1)} u_{1,1}^{(n+1)} + c_{33}^{(n+1)} u_{3,3}^{(n+1)} \\ \text{at } x_3 &= h^{(n)} \\ u_1^{(n)} &= u_1^{(n+1)}, \quad u_3^{(n)} = u_3^{(n+1)} \quad \text{at } x_3 = h^{(n)} \end{aligned} \quad (22)$$

$$\begin{aligned} h^b \bar{c}_{11}^b u_{1,1}^b + c_{55}^{(1)} (u_{3,1}^{(1)} + u_{1,3}^{(1)}) \Big|_{x_3=-h} &= -\rho^b h^b \omega^2 u_1^b \\ \bar{c}_{11}^b u_{1,1}^b &= \bar{e}_{31}^b \bar{V}^b / h^b \quad \text{at } x_1 = 0, 2l \end{aligned} \quad (23)$$

$$\begin{aligned} h^t \bar{c}_{11}^t u_{1,1}^t - c_{55}^{(N)} (u_{3,1}^{(N)} + u_{1,3}^{(N)}) \Big|_{x_3=h} &= -\rho^t h^t \omega^2 u_1^t \\ \bar{c}_{11}^t u_{1,1}^t &= \bar{e}_{31}^t \bar{V}^t / h^t \quad \text{at } x_1 = 0, 2l \end{aligned} \quad (24)$$

$$\begin{aligned} c_{13}^{(1)} u_{1,1}^{(1)} + c_{33}^{(1)} u_{3,3}^{(1)} &= -\rho^b h^b \omega^2 u_3^{(1)}, & u_1^{(1)} &= u_1^b \\ \text{at } x_3 &= -h \\ - (c_{13}^{(N)} u_{1,1}^{(N)} + c_{33}^{(N)} u_{3,3}^{(N)}) &= -\rho^t h^t \omega^2 u_3^{(N)}, & u_1^{(N)} &= u_1^t \\ \text{at } x_3 &= h \end{aligned} \quad (25)$$

2.3. Homogenization of boundary conditions

We transform the inhomogeneous edge conditions in (23) and (24) at end surfaces $x_1 = 0, 2l$ of the actuators into homogeneous conditions by writing

$$\begin{aligned} u_1^b &= \hat{u}_1^b + C^b x_1, & u_1^t &= \hat{u}_1^t + C^t x_1 \\ C^b &= \bar{e}_{31}^b \bar{V}^b / (\bar{c}_{11}^b h^b), & C^t &= \bar{e}_{31}^t \bar{V}^t / (\bar{c}_{11}^t h^t) \end{aligned} \quad (26)$$

and substituting into (23) and (24), which then become homogeneous boundary conditions in \hat{u}_1^b and \hat{u}_1^t at $x_1 = 0, 2l$. In summary, the problem to be analyzed involves solving the following partial differential equations and boundary conditions for $u_1^{(n)}(x_1, x_3)$, $u_3^{(n)}(x_1, x_3)$, $\hat{u}_1^b(x_1)$, and $\hat{u}_1^t(x_1)$:

$$\begin{aligned} c_{11}^{(n)} u_{1,1}^{(n)} + c_{55}^{(n)} u_{1,33}^{(n)} + (c_{13}^{(n)} + c_{55}^{(n)}) u_{3,13}^{(n)} &= -\rho^{(n)} \omega^2 u_1^{(n)} \end{aligned} \quad (27a)$$

$$\begin{aligned} (c_{13}^{(n)} + c_{55}^{(n)}) u_{1,13}^{(n)} + c_{55}^{(n)} u_{3,11}^{(n)} + c_{33}^{(n)} u_{3,33}^{(n)} &= -\rho^{(n)} \omega^2 u_3^{(n)} \end{aligned} \quad (27b)$$

$$c_{11}^{(n)} u_{1,1}^{(n)} + c_{13}^{(n)} u_{3,3}^{(n)} = 0 \quad \text{at } x_1 = 0, 2l \quad (27c)$$

$$u_3^{(n)} = 0 \quad \text{at } x_1 = 0, 2l \quad (27d)$$

$$\begin{aligned} c_{55}^{(n)} (u_{3,1}^{(n)} + u_{1,3}^{(n)}) &= c_{55}^{(n+1)} (u_{3,1}^{(n+1)} + u_{1,3}^{(n+1)}) \\ \text{at } x_3 &= h^{(n)} \\ c_{13}^{(n)} u_{1,1}^{(n)} + c_{33}^{(n)} u_{3,3}^{(n)} &= c_{13}^{(n+1)} u_{1,1}^{(n+1)} + c_{33}^{(n+1)} u_{3,3}^{(n+1)} \\ \text{at } x_3 &= h^{(n)} \\ u_1^{(n)} &= u_1^{(n+1)}, \quad u_3^{(n)} = u_3^{(n+1)} \quad \text{at } x_3 = h^{(n)} \end{aligned} \quad (28)$$

$$\begin{aligned} h^b \bar{c}_{11}^b \hat{u}_{1,1}^b + c_{55}^{(1)} (u_{3,1}^{(1)} + u_{1,3}^{(1)}) \Big|_{x_3=-h} &= -\rho^b h^b \omega^2 (\hat{u}_1^b + C^b x_1) \\ \bar{c}_{11}^b \hat{u}_{1,1}^b &= 0 \quad \text{at } x_1 = 0, 2l \end{aligned} \quad (29)$$

$$\begin{aligned} & h' \bar{c}'_{11} \hat{u}'_{1,11} - c_{55}^{(N)} (u_{3,1}^{(N)} + u_{1,3}^{(N)}) \Big|_{x_3=h} \\ & = -\rho' h' \omega^2 (\hat{u}'_1 + C' x_1) \\ & \bar{c}'_{11} \hat{u}'_{1,1} = 0 \quad \text{at } x_1 = 0, 2l \end{aligned} \quad (30)$$

$$\begin{aligned} & c_{13}^{(1)} u_{1,1}^{(1)} + c_{33}^{(1)} u_{3,3}^{(1)} = -\rho^b h^b \omega^2 u_3^{(1)} \\ & u_1^{(1)} = \hat{u}_1^b + C^b x_1 \quad \text{at } x_3 = -h \\ & - (c_{13}^{(N)} u_{1,1}^{(N)} + c_{33}^{(N)} u_{3,3}^{(N)}) = -\rho' h' \omega^2 u_3^{(N)} \\ & u_1^{(N)} = \hat{u}_1^t + C^t x_1 \quad \text{at } x_3 = h \end{aligned} \quad (31)$$

3. Fourier series solutions

3.1. Plates with actuators on both major surfaces

We assume that the displacements can be expressed as a Fourier series in x_1 . Thus

$$u_1^{(n)} = a_0^{(n)}(x_3) + \sum_{m=1}^{\infty} a_m^{(n)}(x_3) \cos \alpha_m x_1 \quad (32a)$$

$$u_3^{(n)} = \sum_{m=1}^{\infty} b_m^{(n)}(x_3) \sin \alpha_m x_1 \quad (32b)$$

$$\hat{u}_1^b = D_0^b + \sum_{m=1}^{\infty} D_m^b \cos \alpha_m x_1 \quad (32c)$$

$$\hat{u}_1^t = D_0^t + \sum_{m=1}^{\infty} D_m^t \cos \alpha_m x_1 \quad (32d)$$

$$\alpha_m = m\pi/2l \quad (32e)$$

where $a_0^{(n)}(x_3)$, $a_m^{(n)}(x_3)$, $b_m^{(n)}(x_3)$, D_0^b , D_m^b , D_0^t , and D_m^t are to be determined. Equations (32) ensure that all homogeneous boundary conditions at the edges $x_1 = 0$ and $x_1 = 2l$ are satisfied. Substitution of displacement fields (32) into equations (27) yields the following differential equations

$$c_{55}^{(n)} a_{0,33}^{(n)} + \rho^{(n)} \omega^2 a_0^{(n)} = 0 \quad (33)$$

and

$$\begin{aligned} & \lambda_{11}^{(n)} a_m^{(n)} + c_{55}^{(n)} a_{m,33}^{(n)} + \lambda_{12}^{(n)} b_{m,3}^{(n)} = 0 \\ & -\lambda_{12}^{(n)} \alpha_m^{(n)} a_{m,3}^{(n)} + \lambda_{22}^{(n)} b_m^{(n)} + c_{33}^{(n)} b_{m,33}^{(n)} = 0 \end{aligned} \quad (34)$$

where

$$\begin{aligned} & \lambda_{11}^{(n)} = \rho^{(n)} \omega^2 - c_{11}^{(n)} \alpha_m^2 \\ & \lambda_{22}^{(n)} = \rho^{(n)} \omega^2 - c_{55}^{(n)} \alpha_m^2 \\ & \lambda_{12}^{(n)} = (c_{13}^{(n)} + c_{55}^{(n)}) \alpha_m. \end{aligned} \quad (35)$$

The solution to (33) is

$$\begin{aligned} & a_0^{(n)}(x_3) = A_0^{(n)} \cos \eta_0^{(n)} x_3 + \hat{A}_0^{(n)} \sin \eta_0^{(n)} x_3 \\ & \eta_0^{(n)} = (\rho^{(n)} / c_{55}^{(n)})^{1/2} \omega \end{aligned} \quad (36)$$

where $A_0^{(n)}$ and $\hat{A}_0^{(n)}$ are arbitrary constants. In order to find a solution of (34), we let

$$\begin{aligned} & a_m^{(n)}(x_3) = A_m^{(n)} e^{\eta_m^{(n)} x_3} \\ & b_m^{(n)}(x_3) = B_m^{(n)} e^{\eta_m^{(n)} x_3} \end{aligned} \quad (37)$$

where $A_m^{(n)}$, $B_m^{(n)}$ and $\eta_m^{(n)}$ are constants. Substitution of (37) into (34) yields

$$[\lambda_{11}^{(n)} + c_{55}^{(n)} (\eta_m^{(n)})^2] A_m^{(n)} + \lambda_{12}^{(n)} \eta_m^{(n)} B_m^{(n)} = 0 \quad (38a)$$

$$-\lambda_{12}^{(n)} \eta_m^{(n)} A_m^{(n)} + [\lambda_{22}^{(n)} + c_{33}^{(n)} (\eta_m^{(n)})^2] B_m^{(n)} = 0 \quad (38b)$$

which has non-trivial solutions only if

$$\begin{aligned} & [\lambda_{11}^{(n)} + c_{55}^{(n)} (\eta_m^{(n)})^2][\lambda_{22}^{(n)} + c_{33}^{(n)} (\eta_m^{(n)})^2] \\ & + (\lambda_{12}^{(n)})^2 (\eta_m^{(n)})^2 = 0. \end{aligned} \quad (39)$$

Equation (39) can be written as a quadratic equation in $(\eta_m^{(n)})^2$

$$A(\eta_m^{(n)})^4 + B(\eta_m^{(n)})^2 + C = 0 \quad (40)$$

with

$$\begin{aligned} & A = c_{33}^{(n)} c_{55}^{(n)} \\ & B = c_{33}^{(n)} \lambda_{11}^{(n)} + c_{55}^{(n)} \lambda_{22}^{(n)} + (\lambda_{12}^{(n)})^2 \\ & C = \lambda_{11}^{(n)} \lambda_{22}^{(n)} \end{aligned} \quad (41)$$

and $(\eta_m^{(n)})^2$ is given by

$$(\eta_m^{(n)})^2 = \frac{1}{2A} [-B \pm (B^2 - 4AC)^{1/2}] \quad (42)$$

from which the four roots of $\eta_m^{(n)}$ can be easily obtained. The roots can be real or complex conjugate pairs. We label the four roots as $\eta_{mp}^{(n)}$ with $p = 1, 2, 3, 4$. When a particular root with fixed p is real, from (38a) the corresponding solution to (34) can be written as

$$\begin{aligned} & a_m^{(n)}(x_3) = D_{mp}^{(n)} f_{mp}^{(n)}(x_3) \\ & b_m^{(n)}(x_3) = D_{mp}^{(n)} g_{mp}^{(n)}(x_3) \end{aligned} \quad (43)$$

where $D_{mp}^{(n)}$ are arbitrary constants and

$$\begin{aligned} & f_{mp}^{(n)}(x_3) = e^{\eta_{mp}^{(n)} x_3} \\ & g_{mp}^{(n)}(x_3) = -\frac{[\lambda_{11}^{(n)} + c_{55}^{(n)} (\eta_{mp}^{(n)})^2]}{\lambda_{12}^{(n)} \eta_{mp}^{(n)}} e^{\eta_{mp}^{(n)} x_3} \end{aligned} \quad (44)$$

If a pair of complex conjugate roots exist, we denote one of them by $\eta_{mp}^{(n)} = \xi_{mp}^{(n)} + i \zeta_{mp}^{(n)}$ where $\xi_{mp}^{(n)}$ may be zero but $\zeta_{mp}^{(n)}$ is non-zero. Then from (38a) there correspond to this pair of roots two sets of solutions to (34) which can still be written as (43), with

$$\begin{aligned} & f_{mp}^{(n)}(x_3) = \cos \zeta_{mp}^{(n)} x_3 e^{\xi_{mp}^{(n)} x_3} \\ & g_{mp}^{(n)}(x_3) = (\alpha_{11} \cos \zeta_{mp}^{(n)} x_3 + \alpha_{12} \sin \zeta_{mp}^{(n)} x_3) e^{\xi_{mp}^{(n)} x_3} \end{aligned} \quad (45)$$

and

$$f_{mp}^{(n)}(x_3) = \sin \zeta_{mp}^{(n)} x_3 e^{\xi_{mp}^{(n)} x_3} \quad (46)$$

$$g_{mp}^{(n)}(x_3) = (-\alpha_{12} \cos \zeta_{mp}^{(n)} x_3 + \alpha_{11} \sin \zeta_{mp}^{(n)} x_3) e^{\xi_{mp}^{(n)} x_3}$$

respectively, where

$$\alpha_{11} = \frac{1}{(\lambda_{12}^{(n)})^2 [(\xi_{mp}^{(n)})^2 + (\zeta_{mp}^{(n)})^2]} \times \left\{ -\lambda_{12}^{(n)} \xi_{mp}^{(n)} \{ \lambda_{11}^{(n)} + c_{55}^{(n)} [(\xi_{mp}^{(n)})^2 - (\zeta_{mp}^{(n)})^2] \} - 2c_{55}^{(n)} \lambda_{12}^{(n)} \xi_{mp}^{(n)} (\zeta_{mp}^{(n)})^2 \right\}$$

$$\alpha_{12} = \frac{1}{(\lambda_{12}^{(n)})^2 [(\xi_{mp}^{(n)})^2 + (\zeta_{mp}^{(n)})^2]} \times \left\{ -\lambda_{12}^{(n)} \zeta_{mp}^{(n)} \{ \lambda_{11}^{(n)} + c_{55}^{(n)} [(\xi_{mp}^{(n)})^2 - (\zeta_{mp}^{(n)})^2] \} + 2c_{55}^{(n)} \lambda_{12}^{(n)} (\xi_{mp}^{(n)})^2 \zeta_{mp}^{(n)} \right\} \quad (47)$$

We note that there can be at most four specific values of ω which make $B^2 - 4AC = 0$. In that case, (42) has repeated roots for $(\eta_m^{(n)})^2$ and the solution to (34) needs special discussion. We will not consider those special values of ω . In fact, when implemented on a computer, $B^2 - 4AC = 0$ can hardly be exactly true. Hence, the general solution to (34) can be written as

$$a_m^{(n)}(x_3) = \sum_{p=1}^4 D_{mp}^{(n)} f_{mp}^{(n)}(x_3) \quad (48)$$

$$b_m^{(n)}(x_3) = \sum_{p=1}^4 D_{mp}^{(n)} g_{mp}^{(n)}(x_3)$$

Hence we have the following expressions for the solutions to (27a, b)

$$u_1^{(n)} = A_0^{(n)} \cos \eta_0^{(n)} x_3 + \hat{A}_0^{(n)} \sin \eta_0^{(n)} x_3 + \sum_{m=1}^{\infty} \left[\sum_{p=1}^4 D_{mp}^{(n)} f_{mp}^{(n)}(x_3) \right] \cos \alpha_m x_1$$

$$u_3^{(n)} = \sum_{m=1}^{\infty} \left[\sum_{p=1}^4 D_{mp}^{(n)} g_{mp}^{(n)}(x_3) \right] \sin \alpha_m x_1 \quad (49)$$

in which $A_0^{(n)}$, $\hat{A}_0^{(n)}$, and $D_{mp}^{(n)}$ are undetermined constants. The corresponding expressions for the relevant components of the stress tensor are

$$\tau_{11}^{(n)} = \sum_{m=1}^{\infty} \left[\sum_{p=1}^4 D_{mp}^{(n)} h_{mp}^{(n)}(x_3) \right] \sin \alpha_m x_1$$

$$\tau_{33}^{(n)} = \sum_{m=1}^{\infty} \left[\sum_{p=1}^4 D_{mp}^{(n)} l_{mp}^{(n)}(x_3) \right] \sin \alpha_m x_1$$

$$\tau_{31}^{(n)} = -c_{55}^{(n)} A_0^{(n)} \eta_0^{(n)} \sin \eta_0^{(n)} x_3 + c_{55}^{(n)} \hat{A}_0^{(n)} \eta_0^{(n)} \cos \eta_0^{(n)} x_3 + \sum_{m=1}^{\infty} \left[\sum_{p=1}^4 D_{mp}^{(n)} q_{mp}^{(n)}(x_3) \right] \cos \alpha_m x_1 \quad (50)$$

where

$$h_{mp}^{(n)}(x_3) = -c_{11}^{(n)} \alpha_m f_{mp}^{(n)}(x_3) + c_{13}^{(n)} g_{mp,3}^{(n)}(x_3)$$

$$l_{mp}^{(n)}(x_3) = -c_{13}^{(n)} \alpha_m f_{mp}^{(n)}(x_3) + c_{33}^{(n)} g_{mp,3}^{(n)}(x_3) \quad (51)$$

$$q_{mp}^{(n)}(x_3) = c_{55}^{(n)} f_{mp,3}^{(n)}(x_3) + c_{55}^{(n)} \alpha_m g_{mp}^{(n)}(x_3)$$

Substituting (49) and (50) into the continuity conditions (28) at the interface $x_3 = h^{(n)}$, with the orthogonality of the sine and cosine functions, we obtain

$$A_0^{(n)} \cos \eta_0^{(n)} h^{(n)} + \hat{A}_0^{(n)} \sin \eta_0^{(n)} h^{(n)} = A_0^{(n+1)} \cos \eta_0^{(n+1)} h^{(n)} + \hat{A}_0^{(n+1)} \sin \eta_0^{(n+1)} h^{(n)} - c_{55}^{(n)} A_0^{(n)} \eta_0^{(n)} \sin \eta_0^{(n)} h^{(n)} + c_{55}^{(n)} \hat{A}_0^{(n)} \eta_0^{(n)} \cos \eta_0^{(n)} h^{(n)} = -c_{55}^{(n+1)} A_0^{(n+1)} \eta_0^{(n+1)} \sin \eta_0^{(n+1)} h^{(n)} + c_{55}^{(n+1)} \hat{A}_0^{(n+1)} \eta_0^{(n+1)} \cos \eta_0^{(n+1)} h^{(n)} \quad (52)$$

and

$$\sum_{p=1}^4 D_{mp}^{(n)} f_{mp}^{(n)}(h^{(n)}) = \sum_{p=1}^4 D_{mp}^{(n+1)} f_{mp}^{(n+1)}(h^{(n)})$$

$$\sum_{p=1}^4 D_{mp}^{(n)} g_{mp}^{(n)}(h^{(n)}) = \sum_{p=1}^4 D_{mp}^{(n+1)} g_{mp}^{(n+1)}(h^{(n)}) \quad (53)$$

$$\sum_{p=1}^4 D_{mp}^{(n)} q_{mp}^{(n)}(h^{(n)}) = \sum_{p=1}^4 D_{mp}^{(n+1)} q_{mp}^{(n+1)}(h^{(n)})$$

$$\sum_{p=1}^4 D_{mp}^{(n)} l_{mp}^{(n)}(h^{(n)}) = \sum_{p=1}^4 D_{mp}^{(n+1)} l_{mp}^{(n+1)}(h^{(n)})$$

Equations (52) and (53) can be written in the following matrix form

$$\begin{bmatrix} A_0^{(n)} \\ \hat{A}_0^{(n)} \end{bmatrix} = [T]_0^{(n)} \begin{bmatrix} A_0^{(n+1)} \\ \hat{A}_0^{(n+1)} \end{bmatrix} \quad (54)$$

and

$$\begin{bmatrix} D_{m1}^{(n)} \\ D_{m2}^{(n)} \\ D_{m3}^{(n)} \\ D_{m4}^{(n)} \end{bmatrix} = [T]^{(n)} \begin{bmatrix} D_{m1}^{(n+1)} \\ D_{m2}^{(n+1)} \\ D_{m3}^{(n+1)} \\ D_{m4}^{(n+1)} \end{bmatrix} \quad (55)$$

where $[T]_0^{(n)}$ and $[T]^{(n)}$ are two transfer matrices given by

$$[T]_0^{(n)} = \begin{bmatrix} C(\eta_0^{(n)} h^{(n)}) & S(\eta_0^{(n)} h^{(n)}) \\ -c_{55}^{(n)} \eta_0^{(n)} S(\eta_0^{(n)} h^{(n)}) & c_{55}^{(n)} \eta_0^{(n)} C(\eta_0^{(n)} h^{(n)}) \end{bmatrix}^{-1}$$

$$\times \begin{bmatrix} C(\eta_0^{(n+1)} h^{(n)}) & S(\eta_0^{(n+1)} h^{(n)}) \\ -c_{55}^{(n+1)} \eta_0^{(n+1)} S(\eta_0^{(n+1)} h^{(n)}) & c_{55}^{(n+1)} \eta_0^{(n+1)} C(\eta_0^{(n+1)} h^{(n)}) \end{bmatrix} \quad (56)$$

where $C = \cos$ and $S = \sin$, and

$$\begin{aligned} [T]^{(n)} &= \begin{bmatrix} f_{m1}^{(n)}H & f_{m2}^{(n)}H & f_{m3}^{(n)}H & f_{m4}^{(n)}H \\ g_{m1}^{(n)}H & g_{m2}^{(n)}H & g_{m3}^{(n)}H & g_{m4}^{(n)}H \\ q_{m1}^{(n)}H & q_{m2}^{(n)}H & q_{m3}^{(n)}H & q_{m4}^{(n)}H \\ l_{m1}^{(n)}H & l_{m2}^{(n)}H & l_{m3}^{(n)}H & l_{m4}^{(n)}H \end{bmatrix}^{-1} \\ &\times \begin{bmatrix} f_{m1}^{(n+1)}H & f_{m2}^{(n+1)}H & f_{m3}^{(n+1)}H & f_{m4}^{(n+1)}H \\ g_{m1}^{(n+1)}H & g_{m2}^{(n+1)}H & g_{m3}^{(n+1)}H & g_{m4}^{(n+1)}H \\ q_{m1}^{(n+1)}H & q_{m2}^{(n+1)}H & q_{m3}^{(n+1)}H & q_{m4}^{(n+1)}H \\ l_{m1}^{(n+1)}H & l_{m2}^{(n+1)}H & l_{m3}^{(n+1)}H & l_{m4}^{(n+1)}H \end{bmatrix} \end{aligned} \quad (57)$$

where $H = (h^{(n)})$.

With repeated use of (54) and (55), we can obtain the following relations

$$\begin{bmatrix} A_0^{(1)} \\ \hat{A}_0^{(1)} \end{bmatrix} = [T]_0^{(1)} [T]_0^{(2)} \cdots [T]_0^{(N-1)} \begin{bmatrix} A_0^{(N)} \\ \hat{A}_0^{(N)} \end{bmatrix} \quad (58)$$

and

$$\begin{bmatrix} D_{m1}^{(1)} \\ D_{m2}^{(1)} \\ D_{m3}^{(1)} \\ D_{m4}^{(1)} \end{bmatrix} = [T]^{(1)} [T]^{(2)} \cdots [T]^{(N-1)} \begin{bmatrix} D_{m1}^{(N)} \\ D_{m2}^{(N)} \\ D_{m3}^{(N)} \\ D_{m4}^{(N)} \end{bmatrix} \quad (59)$$

With (58) and (59), the interface conditions (28) are satisfied. However, (29)–(31) still remain to be satisfied. We express the non-homogeneous terms $C^b x_1$ and $C^t x_1$ in (29)–(31) by their Fourier series as

$$\begin{aligned} C^b x_1 &= c_0^b + \sum_{m=1}^{\infty} c_m^b \cos \alpha_m x_1 \\ C^t x_1 &= c_0^t + \sum_{m=1}^{\infty} c_m^t \cos \alpha_m x_1 \\ c_0^b &= C^b l \\ c_0^t &= C^t l \\ c_m^b &= \frac{C^b}{l \alpha_m^2} [(-1)^m - 1] \\ c_m^t &= \frac{C^t}{l \alpha_m^2} [(-1)^m - 1] \end{aligned} \quad (60)$$

Substituting from (32c, d), (49), (50), and (60) into (29)–(31), using the orthogonality of the sine and cosine functions, and combining the results with (58) and (59), we obtain the following equations

$$\begin{aligned} (c_{55}^{(1)} \eta_0^{(1)} \sin \eta_0^{(1)} h) A_0^{(1)} + (c_{55}^{(1)} \eta_0^{(1)} \cos \eta_0^{(1)} h) \hat{A}_0^{(1)} \\ + \rho^b h^b \omega^2 D_0^b = -\rho^b h^b \omega^2 c_0^b \end{aligned}$$

$$\begin{aligned} (c_{55}^{(N)} \eta_0^{(N)} \sin \eta_0^{(N)} h) A_0^{(N)} - (c_{55}^{(N)} \eta_0^{(N)} \cos \eta_0^{(N)} h) \hat{A}_0^{(N)} \\ + \rho^t h^t \omega^2 D_0^t = -\rho^t h^t \omega^2 c_0^t \\ (\cos \eta_0^{(1)} h) A_0^{(1)} - (\sin \eta_0^{(1)} h) \hat{A}_0^{(1)} - D_0^b = c_0^b \\ (\cos \eta_0^{(N)} h) A_0^{(N)} + (\sin \eta_0^{(N)} h) \hat{A}_0^{(N)} - D_0^t = c_0^t \\ \begin{bmatrix} A_0^{(1)} \\ \hat{A}_0^{(1)} \end{bmatrix} = [T]_0^{(1)} [T]_0^{(2)} \cdots [T]_0^{(N-1)} \begin{bmatrix} A_0^{(N)} \\ \hat{A}_0^{(N)} \end{bmatrix} \end{aligned} \quad (61)$$

for the six unknowns $A_0^{(1)}$, $\hat{A}_0^{(1)}$, $A_0^{(N)}$, $\hat{A}_0^{(N)}$, D_0^b , and D_0^t , and

$$\begin{aligned} \sum_{p=1}^4 q_{mp}^{(1)}(-h) D_{mp}^{(1)} + (\rho^b h^b \omega^2 - h^b \bar{c}_{11}^b \alpha_m^2) D_m^b \\ = -\rho^b h^b \omega^2 c_m^b \end{aligned}$$

$$\begin{aligned} \sum_{p=1}^4 q_{mp}^{(N)}(h) D_{mp}^{(N)} - (\rho^t h^t \omega^2 - h^t \bar{c}_{11}^t \alpha_m^2) D_m^t \\ = \rho^t h^t \omega^2 c_m^t \end{aligned}$$

$$\sum_{p=1}^4 [l_{mp}^{(1)}(-h) + \rho^b h^b \omega^2 g_{mp}^{(1)}(-h)] D_{mp}^{(1)} = 0$$

$$\sum_{p=1}^4 [-l_{mp}^{(N)}(h) + \rho^t h^t \omega^2 g_{mp}^{(N)}(h)] D_{mp}^{(N)} = 0$$

$$\sum_{p=1}^4 f_{mp}^{(1)}(-h) D_{mp}^{(1)} - D_m^b = c_m^b$$

$$\sum_{p=1}^4 f_{mp}^{(N)}(h) D_{mp}^{(N)} - D_m^t = c_m^t$$

$$\begin{bmatrix} D_{m1}^{(1)} \\ D_{m2}^{(1)} \\ D_{m3}^{(1)} \\ D_{m4}^{(1)} \end{bmatrix} = [T]^{(1)} [T]^{(2)} \cdots [T]^{(N-1)} \begin{bmatrix} D_{m1}^{(N)} \\ D_{m2}^{(N)} \\ D_{m3}^{(N)} \\ D_{m4}^{(N)} \end{bmatrix} \quad (62)$$

for the ten unknowns $D_{mp}^{(1)}$, $D_{mp}^{(N)}$, D_m^b , and D_m^t . Note that $p = 1, 2, 3, 4$. For given ω , equations (61) and (62) are inhomogeneous equations for the forced vibrations of the plate. The vanishing of the coefficient matrix of (62) determines natural frequencies of the system, which lead to resonances if any one of them is close to the forcing frequency ω . We note that from (60) $c_m^b = c_m^t = 0$ when m is even. Hence (62) has non-trivial solutions only when m is odd. This corresponds to vibrations with u_3 being symmetric about $x_1 = l$, the center of the plate.

3.2. Plate with one actuator

For the case of an actuator on only one surface of the plate, for example, on the top, the solution can be simply obtained by replacing the boundary conditions at the

bottom surface of the plate by $\tau_{33}^{(1)} = 0$ and $\tau_{31}^{(1)} = 0$. This results in the following equations

$$\begin{aligned} & (c_{55}^{(1)} \eta_0^{(1)} \sin \eta_0^{(1)} h) A_0^{(1)} \\ & \quad + (c_{55}^{(1)} \eta_0^{(1)} \cos \eta_0^{(1)} h) \hat{A}_0^{(1)} = 0 \\ & (c_{55}^{(N)} \eta_0^{(N)} \sin \eta_0^{(N)} h) A_0^{(N)} - (c_{55}^{(N)} \eta_0^{(N)} \cos \eta_0^{(N)} h) \hat{A}_0^{(N)} \\ & \quad + \rho' h' \omega^2 D_0' = -\rho' h' \omega^2 c_0' \\ & (\cos \eta_0^{(N)} h) A_0^{(N)} + (\sin \eta_0^{(N)} h) \hat{A}_0^{(N)} - D_0' = c_0' \\ & \begin{bmatrix} A_0^{(1)} \\ \hat{A}_0^{(1)} \end{bmatrix} = \begin{bmatrix} T \end{bmatrix}_0^{(1)} \begin{bmatrix} T \end{bmatrix}_0^{(2)} \cdots \begin{bmatrix} T \end{bmatrix}_0^{(N-1)} \begin{bmatrix} A_0^{(N)} \\ \hat{A}_0^{(N)} \end{bmatrix} \end{aligned} \quad (63)$$

for the five unknowns $A_0^{(1)}$, $\hat{A}_0^{(1)}$, $A_0^{(N)}$, $\hat{A}_0^{(N)}$, and D_0' , and

$$\begin{aligned} & \sum_{p=1}^4 q_{mp}^{(1)}(-h) D_{mp}^{(1)} = 0 \\ & \sum_{p=1}^4 q_{mp}^{(N)}(h) D_{mp}^{(N)} - (\rho' h' \omega^2 - h' \bar{c}_{11} \alpha_m^2) D_m' = \rho' h' \omega^2 c_m' \\ & \sum_{p=1}^4 l_{mp}^{(1)}(-h) D_{mp}^{(1)} = 0 \\ & \sum_{p=1}^4 [-l_{mp}^{(N)}(h) + \rho' h' \omega^2 g_{mp}^{(N)}(h)] D_{mp}^{(N)} = 0 \\ & \sum_{p=1}^4 f_{mp}^{(N)}(h) D_{mp}^{(1)} - D_m' = c_m' \\ & \begin{bmatrix} D_{m1}^{(1)} \\ D_{m2}^{(1)} \\ D_{m3}^{(1)} \\ D_{m4}^{(1)} \end{bmatrix} = \begin{bmatrix} T \end{bmatrix}^{(1)} \begin{bmatrix} T \end{bmatrix}^{(2)} \cdots \begin{bmatrix} T \end{bmatrix}^{(N-1)} \begin{bmatrix} D_{m1}^{(N)} \\ D_{m2}^{(N)} \\ D_{m3}^{(N)} \\ D_{m4}^{(N)} \end{bmatrix} \end{aligned} \quad (64)$$

for the nine unknowns $D_{mp}^{(1)}$, $D_{mp}^{(N)}$, and D_m' for each m .

4. An example

As an example, we consider an aluminum plate with PZT-5 actuators on the two major surfaces. For aluminum [7]

$$E = 69 \times 10^9 \text{ N m}^{-2}, \quad \nu = 0.32 \quad \rho = 2700 \text{ kg m}^{-3} \quad (65)$$

and for the PZT-5 [7]

$$\begin{aligned} c_{11}^b &= c_{11}^t = 12.1 \times 10^{10} \text{ N m}^{-2} \\ 7c_{13}^b &= c_{13}^t = 7.52 \\ c_{33}^b &= c_{33}^t = 11.1 \\ e_{31}^b &= e_{31}^t = -5.4 \text{ C m}^{-2} \\ e_{33}^b &= e_{33}^t = 15.8 \\ \rho^b &= \rho^t = 7750 \text{ kg m}^{-3} \end{aligned} \quad (66)$$

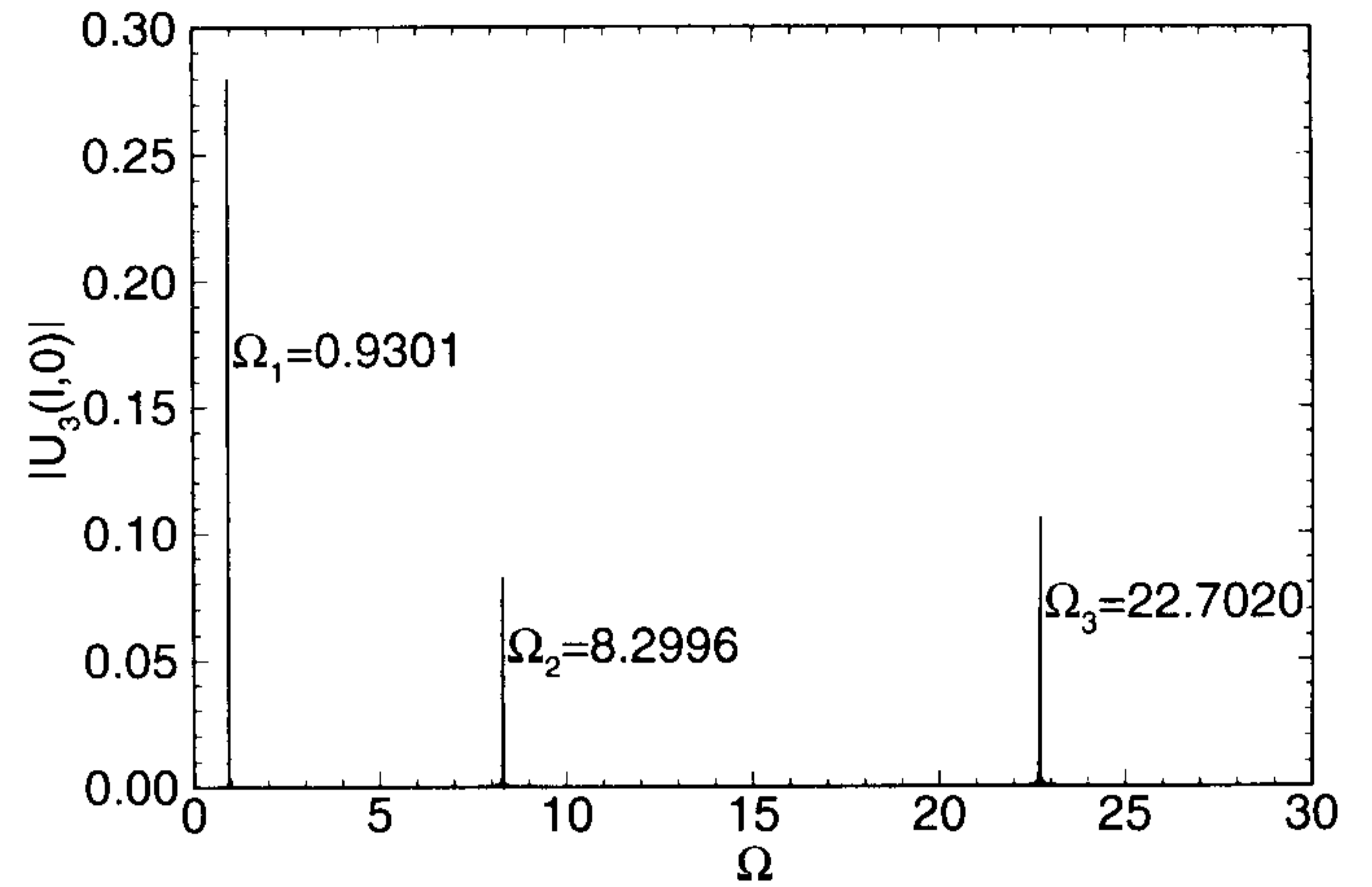


Figure 2. The normalized deflection of the centroid of the plate $|U_3(l, 0)| = |u_3(l, 0)| hc_{31}^p h^b / (2l)^2 e_{31}^p \bar{V}$ as a function of the non-dimensional forcing frequency

$$\Omega = \omega / \frac{\pi^2}{(2l)^2} \left(\frac{EI}{\rho A} \right)^{1/2}$$

For geometric dimensions, we take $2l = 8$ cm, $h = 0.1$ cm, $h^b = h^t = 0.01$ cm. We also set $\bar{V}^b = -\bar{V}^t = 50$ V. Even though the analysis presented above is valid for a laminated elastic plate, in the example considered there is only one lamina. This will facilitate the interpretation of computed results.

The structure has a series of natural bending vibration frequencies which can be ordered according to their magnitudes as $\omega_1, \omega_2, \omega_3, \dots$. The free bending vibration modes corresponding to $\omega_1, \omega_3, \omega_5, \dots$ are symmetric about $x_1 = l$, and those corresponding to $\omega_2, \omega_4, \omega_6, \dots$ are antisymmetric. Only symmetric modes can be excited in our problem because of the symmetry of the structure and the loading conditions. The natural frequencies of the structure can be roughly estimated from the results of the beam theory. When the inertia and rigidity of the actuators are neglected, we have

$$\omega_n \approx \frac{n^2 \pi^2}{(2l)^2} \left(\frac{\bar{E}I}{\rho A} \right)^{1/2} \quad \text{or} \quad \Omega_n = \omega_n / \frac{\pi^2}{(2l)^2} \left(\frac{\bar{E}I}{\rho A} \right)^{1/2} \approx n^2 \quad (67)$$

where $\bar{E}I = \bar{E}(2h)^3/12$ is the flexural rigidity for plane strain deformations of a beam of unit width, $\bar{E} = E/(1 - \nu^2)$, and $A = 2h$ is the cross sectional area. Ω_n is the normalized natural frequency.

We plot the normalized deflection of the centroid of the plate $|U_3(l, 0)| = |u_3(l, 0)| hc_{31}^p h^b / (2l)^2 e_{31}^p \bar{V}$ as a function of the normalized forcing frequency

$$\Omega = \omega / \frac{\pi^2}{(2l)^2} \left(\frac{\bar{E}I}{\rho A} \right)^{1/2}$$

in figure 2. It is seen that $U_3(l, 0)$ becomes large at certain discrete values of ω , which signifies the resonance phenomenon. Those values of Ω at which resonances occur should be in the sequence $\Omega_1, \Omega_3, \Omega_5, \dots$. The values of Ω_1, Ω_3 , and Ω_5, \dots shown in figure 2

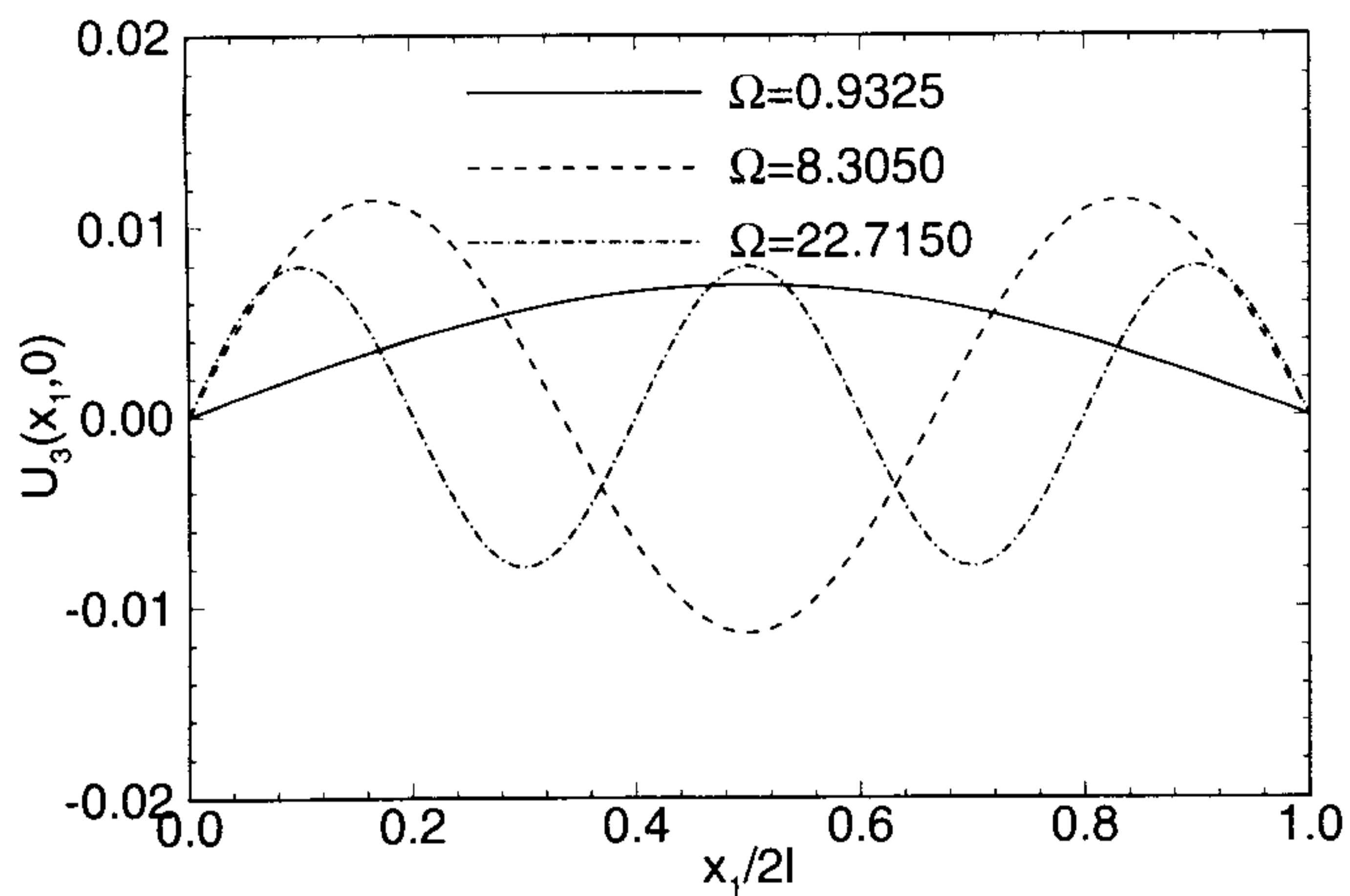


Figure 3. Deflection curves $U_3(x_1, 0)$ for values of Ω near Ω_1 , Ω_3 , and Ω_5 .

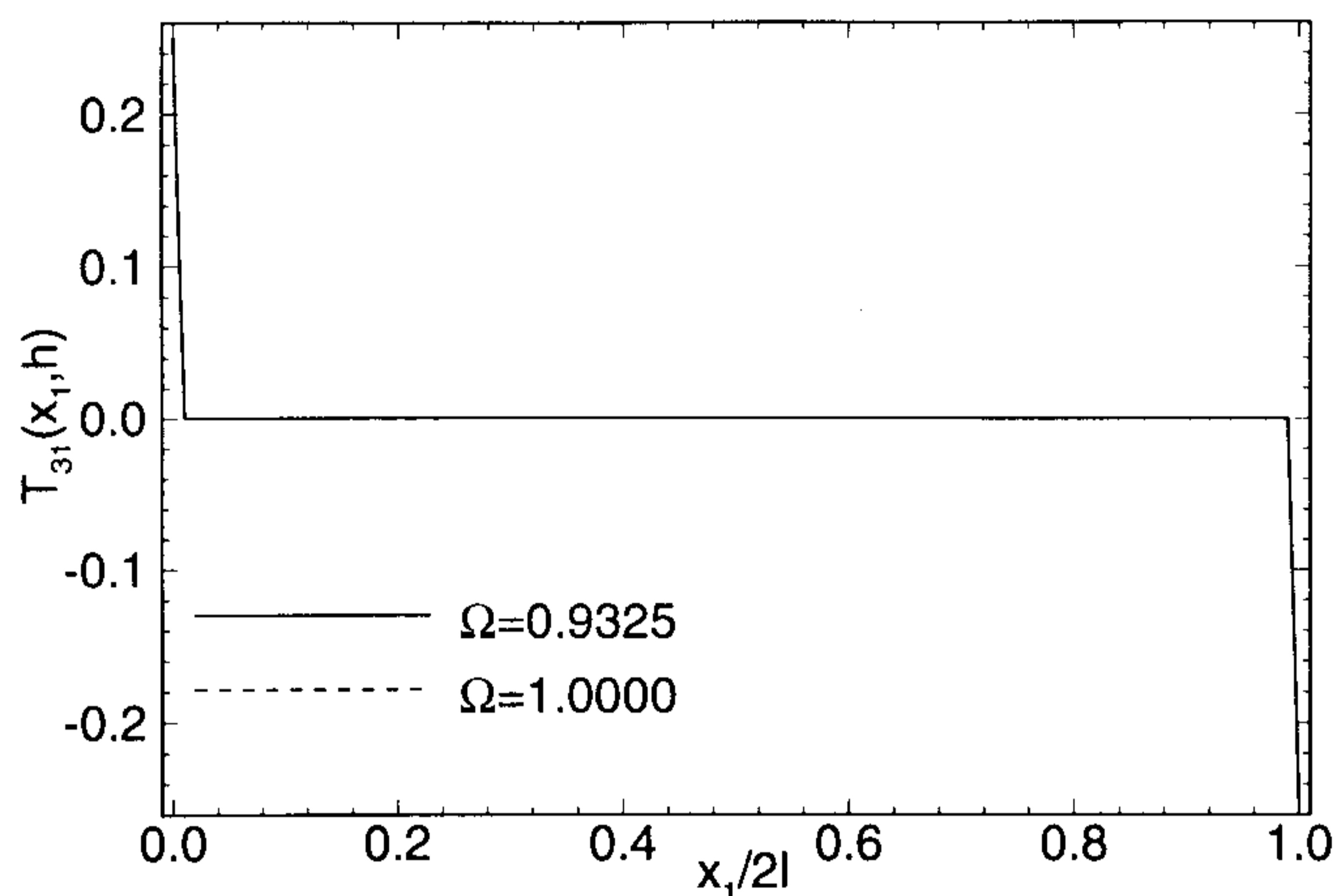


Figure 4. The normalized shear stress $T_{31}(x_1, h) = \tau_{31}(x_1, h)h^b/e_{31}^p \bar{V}$ under the top actuator for values of Ω near Ω_1 .

are $\Omega_1 \approx 0.9301$, $\Omega_3 \approx 8.2996$, and $\Omega_5 \approx 22.7020$ which are close to n^2 , the estimate obtained from the beam theory. In figure 2, only the locations of the peaks that determine the resonant frequencies of the system are important. The relative magnitudes of the peaks depend on how close the sampling points of Ω are to the exact values of Ω_n when the curve is computed.

Normalized deflection curves $U_3(x_1^*, 0) = u_3(x_1, 0) hc_{31}^p h^b / (2l)^2 e_{31}^p \bar{V}$ for values of Ω near the the first three resonance frequencies Ω_1 , Ω_3 , and Ω_5 are plotted in figure 3. The free vibration modes of the plate corresponding to Ω_1 , Ω_3 , and Ω_5 has zero, two, and four nodes respectively. Under a particular forcing frequency Ω , all these modes will be excited. But it can be seen that when Ω is close to a particular resonant frequency, the mode corresponding to that resonant frequency has a dominant contribution to the deflection of the plate. The Fourier series converges very fast. When Ω is near Ω_1 , Ω_3 , or Ω_5 , only five, ten, or twenty terms are needed for $u_3(l, 0)$ to have three significant digits. When Ω is higher, higher order modes also become important hence more terms are needed in the series. For all of the results presented here, 100 terms in the Fourier series are summed to obtain sufficient accuracy.

The normalized shear stress $T_{31}(x_1, h) = \tau_{31}(x_1, h)h^b/e_{31}^p \bar{V}$ at points on the interface between the top actuator and the plate surface for two values of

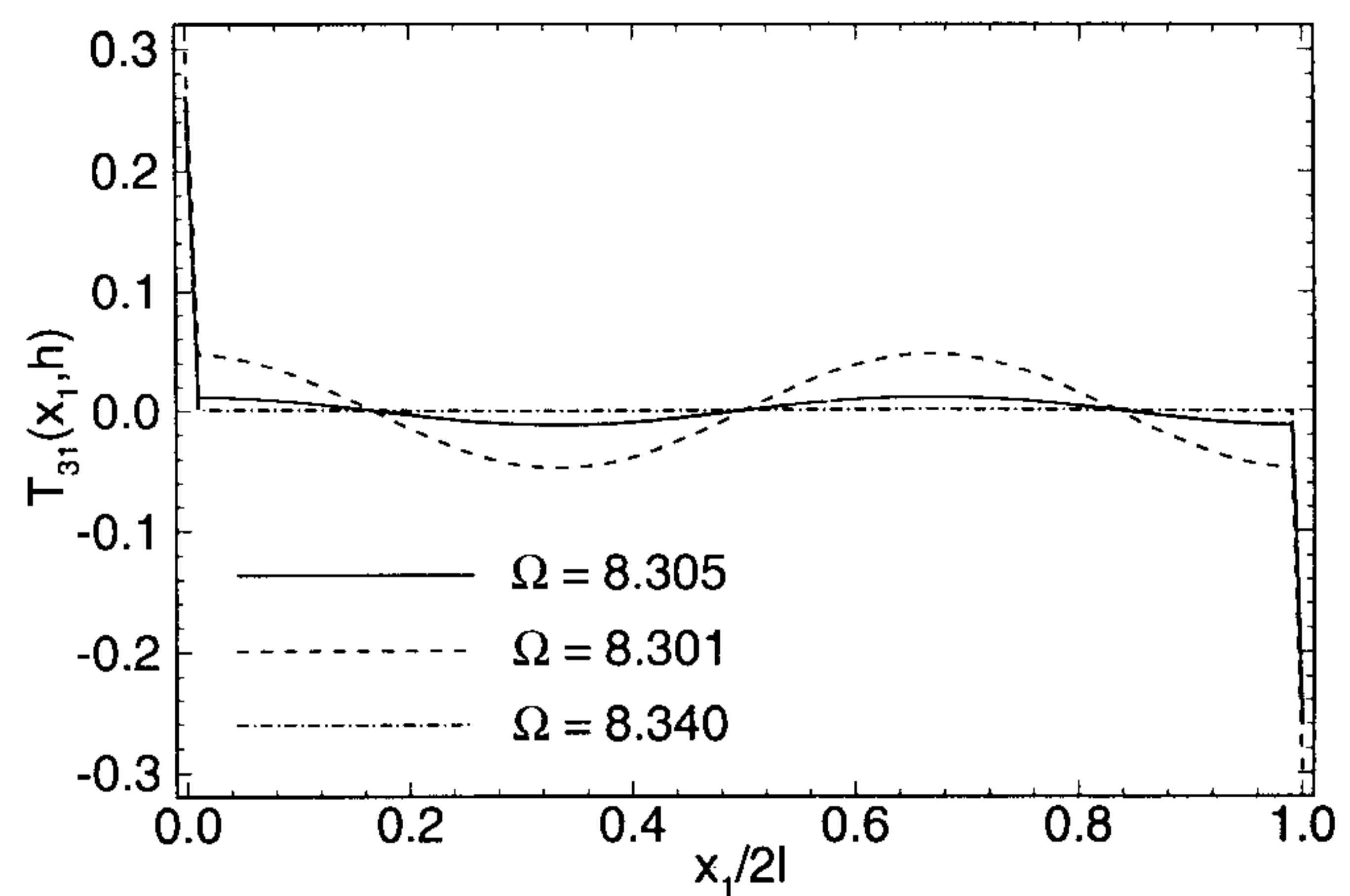


Figure 5. The normalized shear stress $T_{31}(x_1, h)$ under the top actuator for values of Ω near Ω_3 .

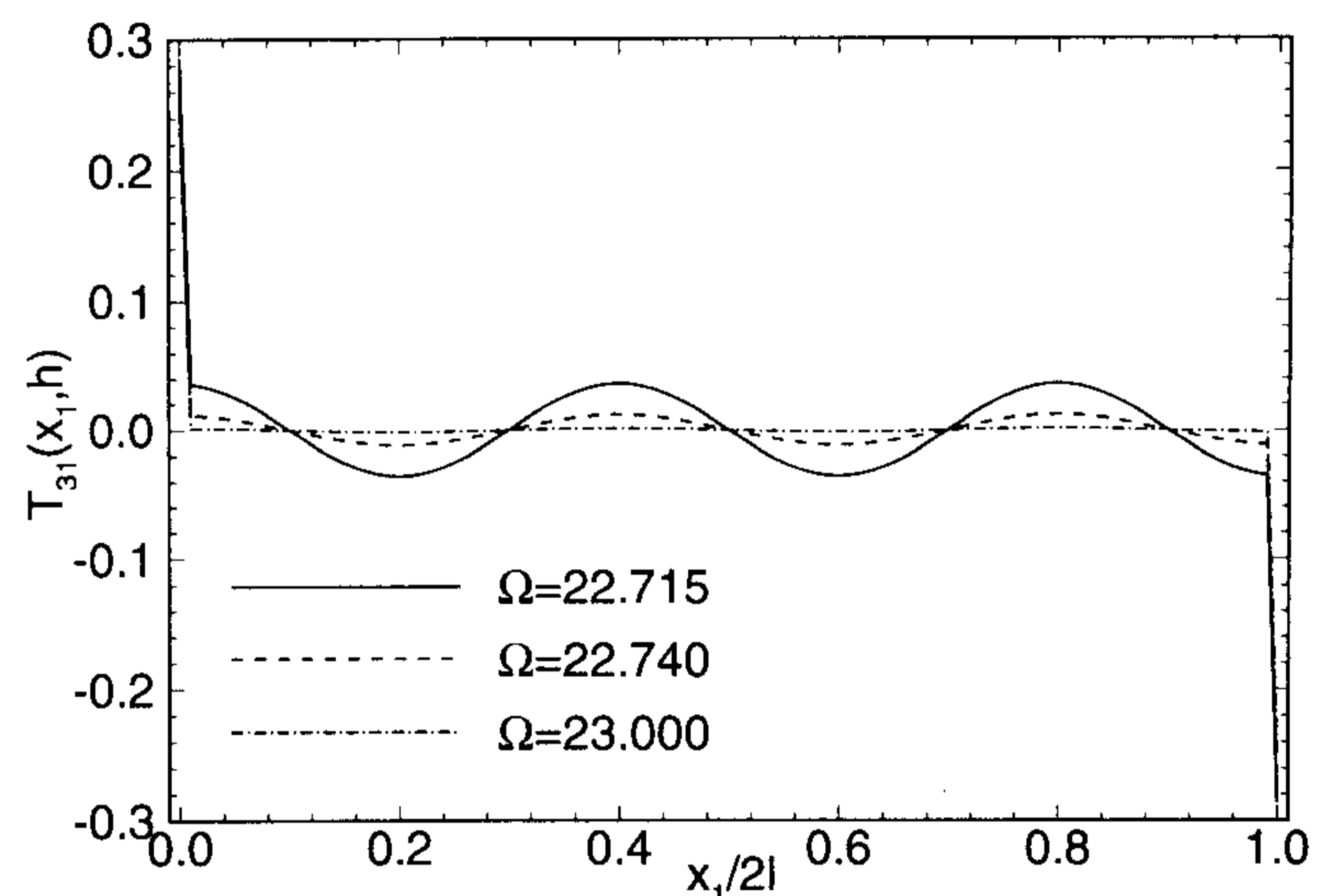


Figure 6. The normalized shear stress $T_{31}(x_1, h)$ under the top actuator for values of Ω near Ω_5 .

Ω around the first natural frequency Ω_1 is plotted in figure 4. The two curves plotted simply overlap and cannot be distinguished from each other. As shown in [5] by the finite element method and in [7] by elasticity theory in static case, the shear stress is non-zero only in the narrow regions near the ends of the actuator. In approximate beam or plate theory, this shear stress has a delta function distribution. The finite element method usually predicts a more gradual change of the shear stress distribution near the ends determined by the element size and interpolation functions [5]. The results by Fourier series sometimes have slight oscillations in the shear stress distribution near the ends [7], which look like the Gibbs phenomenon of a Fourier series near a jump discontinuity. In our case, when the number of terms summed in the Fourier series is equal to the number of equally spaced sampling points in x_1 -direction (100 points in this example), the oscillations do not show up.

The normalized shear stress $T_{31}(x_1, h)$ under the top actuator for values of Ω around the third natural frequency Ω_3 is plotted in figure 5. It is seen that when Ω is not very close to Ω_3 , the qualitative behavior of the shear stress distribution is similar to that shown in figure 4. But when Ω gets very close to Ω_3 , the shear stress is no longer zero in the central portion of the plate and shows a sinusoidal variation which

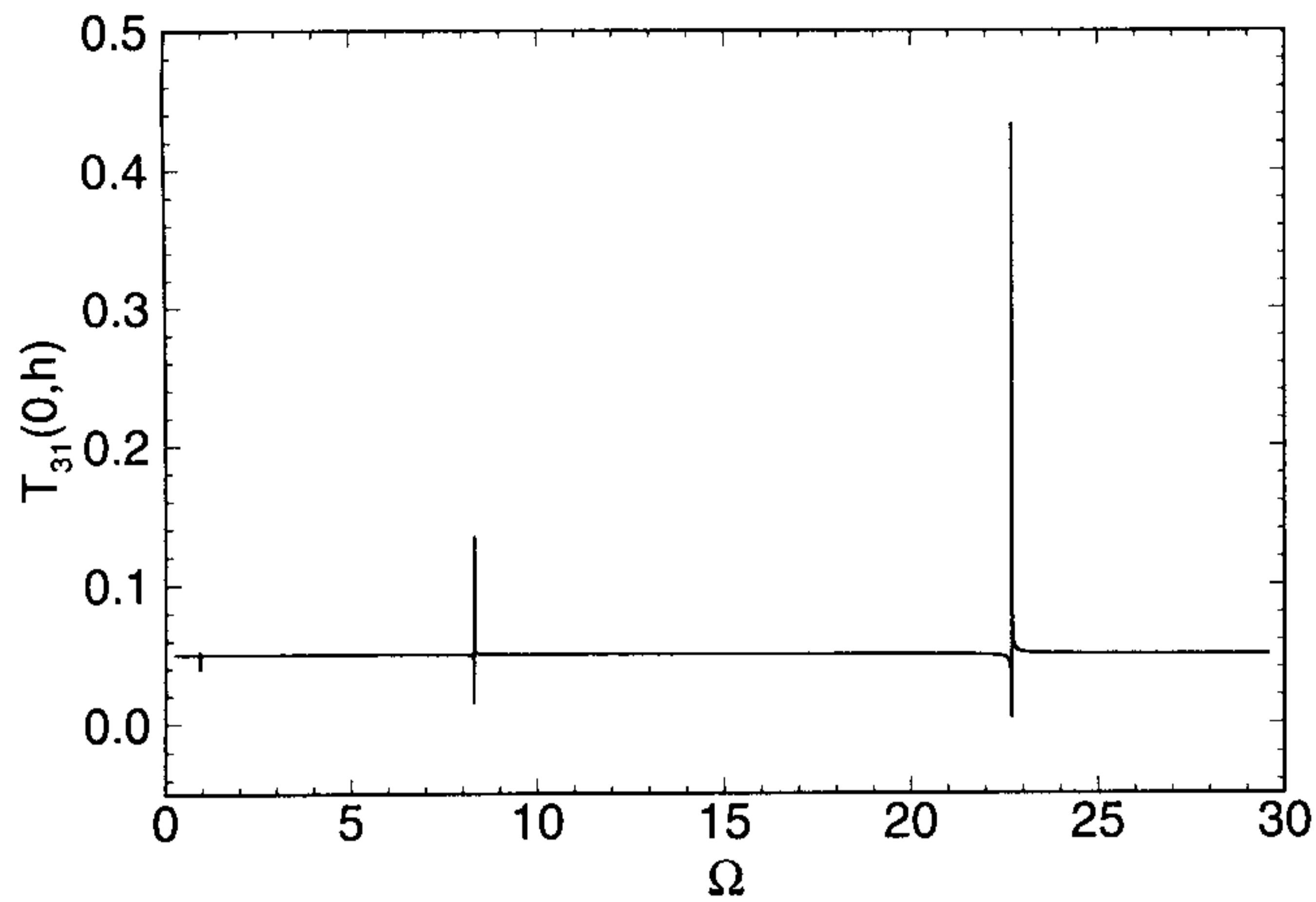


Figure 7. The maximum normalized shear stress $T_{31}(0, h)$ as a function of Ω .

seems to be related to the deflection of the plate. When Ω is very close to Ω_3 , resonance occurs and the deformations of the plate may get large. In that case a non-linear analysis with finite deformation theory is needed. Similar behavior of the shear stress distribution is observed when Ω is around Ω_5 and is plotted in figure 6.

Finally, maximum normalized shear stress $T_{31}(0, h)$ under the left end of the top actuator as a function of Ω is plotted in figure 7. The maximum normalized shear stress is almost constant for various values of Ω except when Ω is very close to a natural frequency Ω_n .

5. Conclusions

We have presented a Fourier series analysis of the cylindrical bending vibration of a laminated elastic plate forced by piezoelectric actuators under time harmonic electric voltage. The solution is exact within the assumptions of plane strain deformations and elasticity theory. The Fourier series converges rapidly in the numerical example studied. For the aluminum plate with actuators attached to its top and bottom surfaces, it is shown that the normalized shear stress is essentially zero except in very small regions near the two edges,

and except for a forcing frequency close to one of the natural frequencies of the plate. In the latter case, the shear stress at the contact surface between the actuator and the plate is non-zero almost everywhere. The computed natural frequencies are found to be close to those estimated from the beam theory. We note that the solution obtained by the method of Fourier series may exhibit Gibbs phenomenon at a free end of a plate.

Acknowledgments

This work was supported by the US Army Research Office grant DAAH 04-93-G-0284 to the University of Missouri-Rolla, and a matching grant from the Missouri Research and Training Center.

References

- [1] Chaudhry Z A and Rogers C A 1992 A mechanics approach to induced strain actuation of structures *Proc. 3rd Int. Conf. on Adaptive Structures (San Diego, CA)*
- [2] Pagano N L 1969 Exact solutions for composite laminates in cylindrical bending *J. Comp. Mats.* **3** 398–411
- [3] Ray M C, Rao K M and Samanta B 1992 Exact analysis of coupled electroelastic behavior of a piezoelectric plate under cylindrical bending *Computers and Structures* **45** 667–77
- [4] Ray M C, Rao K M and Samanta B 1993 Exact solution for static analysis of an intelligent structure under cylindrical bending *Computers and Structures* **47** 1031–42
- [5] Zhou Y S and Tiersten H F Elastic analysis of laminated composite plates in cylindrical bending due to piezoelectric actuators *Smart Mater. Struct.* **3** 255–65
- [6] Tiersten H F 1993 Electroelastic equations for electroded thin plates subject to large driving voltages *J. Appl. Phys.* **74** 3389–93
- [7] Hanagud S and Kulkarni G 1992 Coupled piezoceramic–elastic structures with finite deformations *Developments in Theoretical and Applied Mechanics (Proc. 16th Southeastern Conference on Theoretical and Applied Mechanics)* ed B Antar, R Engels, A A Prinaris and T H Moulden (University of Tennessee Space Institute) vol XVI pp II.20.22–30